PROTEIN SEQUENCE DOMAIN ANNOTATION USING LANGUAGE MODELS

Anonymous authors
Paper under double-blind review

ABSTRACT

Protein function inference relies on annotating protein domains via sequence similarity, often modeled through profile Hidden Markov Models (profile HMMs), which capture evolutionary diversity within related domains. However, profile HMMs make strong simplifying independence assumptions when modeling residues in a sequence. Here, we introduce PSALM (Protein Sequence Annotation using Language Models), a hierarchical approach that relaxes these assumptions and uses representations of protein sequences learned by protein language models to enable high-sensitivity, high-specificity residue-level protein sequence annotation. We also develop the Multi-Domain Protein Homology Benchmark (MDPH-Bench), a benchmark for protein sequence domain annotation, where training and test sequences have been rigorously split to share no similarity between any of their domains at a given threshold of sequence identity. Prior benchmarks, which split one domain family at a time, do not support methods for annotating multi-domain proteins, where training and test sequences need to have multiple domains from different families. We validate PSALM's performance on MDPH-Bench and highlight PSALM as a promising alternative to HMMER, a state-of-the-art profile HMM-based method, for protein sequence annotation.

1 INTRODUCTION

Proteins are composed of distinct structural and functional units conserved through evolution, known as domains. The primary aim of protein sequence annotation is to locate and characterize these domains within a given sequence. Insight into the individual functions of these domains, which may act independently or in concert with neighboring domains, may shed light on the overall biological role of the protein (Fig. 1). Since experimental characterization of protein function can be difficult, function is often inferred and annotated through sequence similarity (homology) to domains with known function (Pearson, 2013; Eddy, 1998). As the size of protein sequence databases and the number of protein sequences with unknown function continue to grow rapidly (UniProt Consortium, 2023), methods for large-scale sequence annotation are essential for exploiting this wealth of information to understand the molecular basis and evolutionary trajectory of life.

Large-scale annotation differs from a typical homology search, where a query protein sequence of interest is searched against a database of many millions of other protein sequences. There are many, varied approaches to identifying homologous *sequences* including both structure-based methods, like Foldseek (Van Kempen et al., 2024), and sequence-based methods, like JackHMMER (Johnson et al., 2010; Eddy, 2011), a profile hidden Markov model (profile HMM)-based approach, and pLM-BLAST (Kaminski et al., 2023), a protein language model (pLM)-based approach. However, annotation involves more than simply identifying similar sequences; it requires linking those similarities to specific families of domains with known function. The state of the art in protein domain sequence annotation uses profile HMMs to detect domains (Eddy, 2011) and profile/profile comparison to identify homologous domains (Remmert et al., 2012). Databases of protein domain families, like Pfam (Mistry et al., 2021), categorize millions of protein sequences into approximately 20,000 domains. Annotation can be achieved by using databases of protein families to compare a protein sequence against 20,000 predefined domain profiles rather than scanning against millions of individual sequences, a strategy that is well-suited for large-scale annotation tasks. Domain-based annotation goes beyond classifying the whole protein sequence; it identifies the domain composition as well as the boundaries of each domain. This "domain annotation" requires annotation at the residue level,

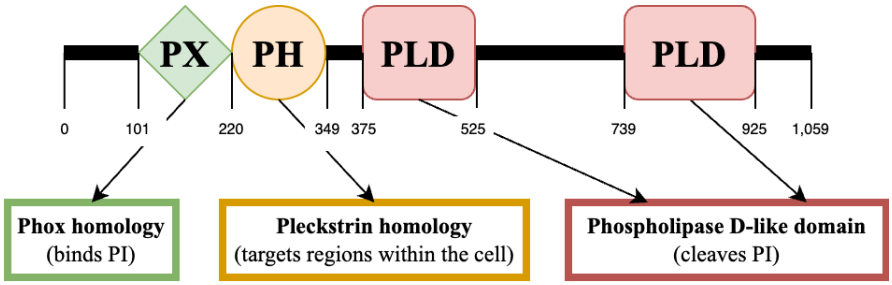

Figure 1: **Annotated domain architecture of a human phospholipase D1 protein** (Q59EA4) (EMBL-EBI, 2024; Paysan-Lafosse et al., 2023), featuring PX (phox), PH (pleckstrin homology), and PLD (phospholipase D-like) domains. Together, the function of these domains suggest that the full length protein (1,059 amino acids) is involved in phosphatidylcholine (PI) cleavage and intracellular signaling, consistent with experimental evidence.

labeling each amino acid symbol in the sequence. Domain annotation helps with function inference and avoids the "transitive annotation catastrophe", where sequence-level annotations inferred from the presence of one domain can erroneously transfer between sequences due to homology of an unrelated domain (Doerks et al., 1998).

Profile HMMs make simplifying independence assumptions when modeling residues in protein sequences that may limit their ability to recognize more subtle, long-range dependencies between residues, potentially reducing sensitivity to distant evolutionary relationships. While deep learning-based methods have been explored as a more sensitive alternative, most focus on whole-protein or single-domain classification (Bileschi et al., 2022; Heinzinger et al., 2022; Nallapareddy et al., 2023; Kaminski et al., 2023; Hamamsy et al., 2023), they do not address the challenge of identifying individual domain subsequences within longer target sequences, which requires careful benchmarking and data curation to assess performance.

In this work, we introduce Protein Sequence Annotation with Language Models (PSALM), a novel approach that extends the capabilities of ESM-2, a pre-trained protein language model (pLM) (Lin et al., 2023), to predict *residue-level* sequence annotations. Our contributions include:

- **First deep learning model for residue-level protein domain annotation:** PSALM is the first deep learning approach to annotate domain boundaries and subsequences within multidomain proteins.
- **Relaxation of HMM independence assumptions for improved sensitivity and specificity:** PSALM leverages pLMs to overcome the simplifying assumptions of profile HMMs, allowing for greater sensitivity in detecting conserved domains across distantly-related sequences and higher specificity in identifying previously unannotated domains.
- **First benchmark for multi-domain protein annotation, MDPH-Bench:** To enable robust evaluation, we introduce the Multi-Domain Protein Homology Benchmark (MDPH-Bench). This benchmark rigorously curates training and test sets to prevent any domain similarity above a predefined threshold, enabling realistic assessments of model performance across diverse domain families and multidomain proteins, which previous benchmarks do not support.

2 Related Work

2.1 Profile HMMs

Profile HMMs use curated multiple sequence alignments (MSAs) of related domains, which reveal patterns of conservation and variability at the residue level, to model consensus using "match", "insert", and "delete" hidden states (Durbin et al., 1998; Eddy, 1998). These models serve as templates for comparison against the sequence of interest, enabling the identification of domains by finding subsequences that match the profile HMMs. Sequences with multiple, unrelated domains will

require the use of multiple profile HMMs for annotation. HMMER (Eddy, 2011) is the state-of-the-art protein sequence domain annotation method and underlies many different databases, which organize related domains into MSAs and profile HMMs at varying levels of granularity, enabling profile-based annotations at the superfamily (Pandurangan et al., 2019), family (Mistry et al., 2021), and sub-family (Thomas et al., 2022) levels. While profile HMMs have enabled sensitive, high-coverage, large-scale annotation of the known protein universe (Mistry et al., 2021), they make two limiting assumptions. Profile HMMs assume both that the observed residues are conditionally independent given the hidden state and that the transition to the next hidden state depends only on the current state (Markov property). While these assumptions simplify the modeling process, they may prevent profile HMMs from capturing complex dependencies between residues in a sequence by ignoring how residues distant in the one-dimensional sequence can interact with each other, especially over long distances, in the folded three-dimensional structure of the protein.

2.2 Deep Models

Recent breakthroughs like AlphaFold2 (Jumper et al., 2021) prove that deep-learning-based approaches can learn these complex relationships from sequence data. However, efforts to apply deep learning methods to predict protein function from sequence have either focused on predicting ontology-based functional annotation at the sequence level (Cao & Shen, 2021; Hong et al., 2020; Kulmanov & Hoehndorf, 2020; Sanderson et al., 2023) or recognizing homology at the sequence level (Heinzinger et al., 2022; Nallapareddy et al., 2023; Kaminski et al., 2023; Hamamsy et al., 2023). To our knowledge, ProtENN, an ensemble of convolutional neural networks, represents the first attempt to predict Pfam domains directly from protein sequences (Bileschi et al., 2022). ProtENN, however, is constrained to make one domain prediction per input sequence and cannot natively identify domain boundaries or multiple domains within a sequence without ad hoc post-processing. Additionally, ProtENN cannot provide information on the contribution of an individual residue to a predicted annotation.

3 Methods

3.1 Problem Formulation

Here, we formalize the residue-level sequence annotation problem as a mapping from a protein sequence $\mathbf{x} = (x_1, x_2, \ldots, x_L)$ to a sequence of protein domain families $\mathbf{y} = (y_1, y_2, \ldots, y_L)$. For residue i in a sequence, x_i is an index $1 \ldots 25$ representing the i-th amino acid character (20 canonical, 2 non-canonical, and 3 ambiguous amino acid characters), and y_i is an index $1 \ldots D$ representing the i-th protein domain family annotation, with $D + 1$ for none. Approximately 23% of protein sequences and 47% of residues across all sequences in UniProt do not belong to any Pfam domain family (Mistry et al., 2021). The goal of residue-level annotation is to learn a model that predicts domain family annotations for each residue in a protein sequence:

$$\hat{y}_i = \arg\max_f P(Y_i = f|\mathbf{x}), \tag{1}$$

where $P(Y_i)$ is the distribution over $D + 1$ family annotations for a given residue i.

3.2 Protein Language Model

Numerically encoding protein sequences is necessary as an input for machine learning tasks such as classification. Protein language models (pLMs) learn vector representations of both individual residues and full-length protein sequences, which capture long-range interactions, predict function via transfer learning, and achieve state-of-the-art performance in several structure prediction tasks Bepler & Berger (2021); Rao et al. (2020); Meier et al. (2021); Elnaggar et al. (2021). We use ESM-2 (specifically, the 8M, 35M, 150M, and 650M parameter models), a pre-trained general-purpose pLM (Lin et al., 2023), to generate residue-level sequence embeddings $\mathbf{x}'$ for a given sequence $\mathbf{x}$. ESM-2 was trained using a BERT-style masked token prediction task (Devlin et al., 2018), enabling it to capture contextual information and dependencies within protein sequences and allowing us to replace $\mathbf{x}$ with $\mathbf{x}'$.

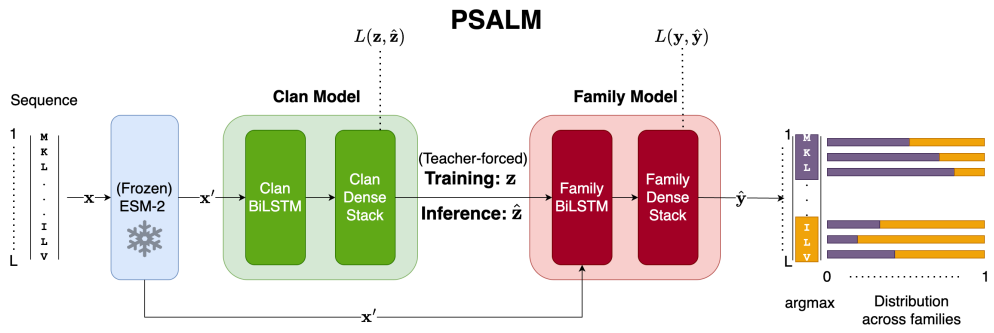

Figure 2: **Overview of residue-level protein sequence annotation with PSALM.** A sequence $\mathbf{x}$ of length L is embedded as $\mathbf{x}'$ with a frozen ESM-2. The PSALM clan and family models predict the clan annotations $\hat{\mathbf{z}}$ and family annotations $\hat{\mathbf{y}}$, respectively, and are trained to minimize cross-entropy loss $L(\cdot)$. During training only, the true clan annotations $\mathbf{z}$ are provided to the family model. Here, the example outputs are predicted across a set of 2 families.

3.3 PSALM

We introduce PSALM (Protein Sequence Annotation using Language Models), a method to predict domains across a protein sequence at the residue-level (Fig. 2). PSALM uses a hierarchical approach that considers both individual protein domain families and clans, which are collections of evolutionarily related (homologous) protein domain families categorized by Pfam (Finn et al., 2006). In Pfam 35.0, approximately 45% of the 19,632 Pfam families are grouped into 655 clans, and a family can only belong to at most one clan. While our primary aim is to predict protein domain families at each residue, modeling clans – the super class – is an interpretable intermediate step that aids in identifying areas of functional or structural importance that may not have clear family-level annotations.

This intermediate annotation problem is a mapping from $\mathbf{x}$ to a sequence of Pfam clans $\mathbf{z} = (z_1, z_2, \ldots, z_L)$, where z_i is an index $1 \ldots C$ representing the i-th clan annotation, with $C + 1$ for "non-clan" or $C + 2$ for none. The non-clan annotation describes a residue which belongs to a domain family that is not a member of clan, and none refers to a residue which does not belong to a domain family and thus does not belong to a clan. For a given residue, the PSALM clan and family models learn to predict:

$$\hat{z}_i = \arg\max_c P(Z_i = c|\mathbf{x}') \tag{2}$$

$$\hat{y}_i = \arg\max_f P(Y_i = f|Z_i = C(f), \mathbf{x}')P(Z_i = C(f)|\mathbf{x}'), \tag{3}$$

where $C(f)$ is the clan label to which family f belongs, and $P(Z_i)$ is the distribution over all $C + 2$ clan annotations for a given residue i. The inclusion of a separate clan prediction task ensures the interpretability of the clan model, preventing it from becoming an abstract hidden state. The family model is trained via the teacher forcing algorithm (Williams & Zipser, 1989), where it is provided the correct clan annotation for each residue in order to mitigate error propagation.

The clan and family models follow a similar structure and are trained separately. Protein sequences are initially embedded at the residue level using a pre-trained and frozen instance of ESM-2, providing a sequence of continuous, context-dependent residue-level embeddings as a replacement for the sequence of amino acid characters typically used as input to profile HMMs. The resulting embeddings are then passed into a single bidirectional Long Short-Term Memory (BiLSTM) layer to capture sequential dependencies (Hochreiter & Schmidhuber, 1997) in the forwards and backwards directions. This bidirectional approach was chosen to mimic the backward pass in profile HMM optimization, aligning with their ability to account for sequence contexts in both directions (Eddy, 1998). RNNs, including BiLSTMs, have been shown to generalize profile HMMs by extending their capacity to model complex, nonlinear dependencies in sequential data, while retaining state-based representations (Wessels & Omlin, 2000; Salaün et al., 2019). The choice of BiLSTM was made deliberately to

introduce as few changes as possible, ensuring that the observed performance improvements could be attributed primarily to the use of the protein language model, rather than architectural differences from profile HMMs. The output from the BiLSTM layer is subsequently decoded using a stack of three dense layers, scaled to the number of clans or family labels, to produce logits across the prediction space. Probabilities are computed by applying softmax to the logits generated by each model.

4 BENCHMARK

In many machine learning contexts, data samples are often assumed to be independent instances drawn from a distribution of the data, justifying random training-test splits. However, this assumption does not hold for sequences in protein domain families, which share evolutionary relationships. Random data splits for protein sequences may lead to performance overestimation, motivating the need to explicitly consider sequence similarity when partitioning data into distinct training and test sets (Söding & Remmert, 2011; Walsh et al., 2016; Jones, 2019; Walsh et al., 2021; Petti & Eddy, 2022). For MDPH-Bench, we aim to create a benchmark that simulates the challenges posed by the remote homology detection problem, where previously unknown or unannotated sequences with little similarity to the training set are especially difficult to detect and annotate. To address this, the MDPH-Bench test set includes a diverse selection of multi-domain proteins, spanning a wide range of sequence similarity to the training set.

4.1 BENCHMARK CREATION

The goal of benchmark creation is performed in two phases. In the first phase, we filter *domains* by a strict sequence percent identity (PID; Appendix A.1.1) to remove similar domains and ensure that test domains are sufficiently dissimilar from training domains. In the second phase, we retrieve the *full-length* sequences corresponding to these domains and categorize them by their similarity to the training set. We begin by collecting the 1.2M "seed domains" from Pfam-A Seed 35.0, a set of curated, representative domains for each domain family that are used to build the 20K Pfam profile HMMs (Mistry et al., 2021). We apply BLUE (Petti & Eddy, 2022), a graph-based sequence splitting algorithm, to partition the seed domains into preliminary training and test sets, defining an edge between two domains as their pairwise PID)Appendix A.1.1). We choose a PID threshold of 25% to split the seed domains as a meaningful cutoff to differentiate structurally and functionally distinct domains – protein pairs that share >25% identity indicate similar structure and function (Sander & Schneider, 1991), and less than 1-% of protein pairs sharing <25% identity have similar structures (Rost, 1999). This filtering step results in 560K training domains and 190K test domains. The remaining 450K seed domains were discarded due to sharing $> 25\%$ PID with both test and training sets.

In order to effectively assess the ability of PSALM to identify multiple domains in a sequence (as opposed to annotating a pre-determined region of interest), the benchmark needs to contain *full-length* protein sequences. We retrieve the full-length sequences corresponding to these representative training and test domains from UniProt release March 2021, a comprehensive database of 230M protein sequences. This results in 517K training sequences. From the test set, we eliminate duplicate sequences also present in the training set. All sequences across both training and test sets are annotated via the `hmmscan` tool from HMMER (Eddy, 2011) with strict inclusion thresholds (E-value < 0.001, bitscore $\geq$ 30) in order to identify domain hits that constitute a "ground truth", with special care to nested, contiguous domains, which may escape typical processing methods (Appendix A.1.2). For training and test purposes, family and clan labels are only assigned to ground truth domains. We discard sequences in test that do not contain an annotated ground truth domain represented by at least 20 ground truth domains from the same family in the training set, resulting in 73K test sequences.

Simply splitting domains by PID is not sufficient to enforce the same gaurantees on full-length, multi-domain proteins, as the full-length sequences may contain additional domains beyond the seed domains. Thus, we further categorize each retrieved test sequence by the maximum PID that any of its domains shares with any domain in the training set as a conservative proxy for its distance from the training set (Appendix A.1.3). We partition the test set into five subsets based on this maximum PID (Table 1), and a total of 6K validation sequences are sampled uniformly across the test subsets. Such a partition may result in test sequences that, for example, may be placed in the $80 <$ PID ≤ 100

Table 1: MDPH-Bench test subset, training, and validation details

Test splits	0-20%	20-40%	40-60%	60-80%	80-100%	Train	Val
Sequences	4,087	37,319	17,446	8,570	5,864	517,936	5,775
Families	543	2,456	1,952	1,731	1,697	14,811	2,097
Clans	180	414	365	341	319	646	388
Coverage	65.31%	59.74%	58.66%	62.02%	56.71%	60.41%	58.79%
Average PID	18.35%	27.64%	42.45%	58.08%	80.01%	NA	45.08%

subset due to a single domain closely related to one in the training set, whereas the test sequence may have several other domains that share significantly lower PID with domains in the training set (this is why the average PID is near the lower bound of the max PID range for many of the test subsets in Table 1). The domain coverage, defined as the average percent of residues in a sequence that are labeled by Pfam domains, is similar across all test subsets.

4.2 Addressing Possible Leakage

We address the potential for unannotated domains to introduce data leakage across the training and test sets by shuffling all subsequences without family and clan labels in the test sequences to disrupt possible domain structures, preserving 0^{th} order residue-composition (Pearson, 2013; Eddy, 2011). The ground truth for protein sequence annotation is fundamentally unknown, relying on inference rather than complete structural and evolutionary knowledge – this is why we must assume natrual sequences contain unannotated true domains that new methods may discover. Since PSALM may be sensitive enough to identify unannotated domains, it is trained with these regions shuffled, to mitigate penalties for "false positives" (with respect to the ground truth annotations). Another source of data leakage may arise from the millions of representative sequences from the UniRef50 database release April 2021 (Suzek et al., 2015) used to train ESM-2. We identify that none of the 4,087 sequences in the $0 < \text{PID} \leq 20$ test subset were present as representative sequences in this version of UniRef50. However, UniRef50 may contain close homologs to the sequences in this test subset.

5 Results

5.1 Baselines

We establish four baseline methods for comparison. We use HMMER, the current state-of-the-art protein sequence annotation method, to build profile HMMs from MSAs of the ground truth domains in the training set, denoted as HMMER*, and use these profiles to annotate the test sequences with `hmmscan`. This allows us to evaluate how a state-of-the-art profile HMM method compares to PSALM when using the same training and testing sets. Additionally, we implement three variants of PSALM, denoted as PSALM_{OH}, where one-hot embeddings for each amino acid in a protein sequence are utilized instead of embeddings from the pre-trained protein language model ESM-2, PSALM_{F}, where the intermediate clan annotations are ommitted, leaving only a PSALM family model with no clan priors, and PSALM_{FF} (prompted by a reviewer), where the BiLSTM components of both the clan and family models are removed, leaving just the FFNN. These comparisons help discern whether differences in performance between PSALM and HMMER* are influenced more by the ESM-2 embeddings, intermediate clan predictions, or by the subsequent neural network architecture.

More recent deep learning approaches (e.g., ProtENN) are not included as baselines because they address sequence-level or single-domain classification, which is a different problem that is largely irrelevant to domain- or residue-level annotation. We discuss the difference between the two in our related work section (Section 2.2). Biologists prefer domain-level annotation for many reasons, including avoiding the "transitive annotation catastrophe", where unrelated sequences cluster through homologous domains (e.g., protein AB shares homology with BC, BC with CD, and all three cluster; but AB shares no homology with CD) (Doerks et al., 1998; Ponting & Birney, 2005; Dawson et al., 2017). Biologists rely on extensive domain-level annotation resources built on a state of the art of profile HMMs (Mistry et al., 2021; Paysan-Lafosse et al., 2023).

Model	# Params		Learning Rate	
	Clan	Family	Clan	Family
PSALM_{650}	69M	166M	5e−4	5e−5
PSALM_{150}	18M	67M	5e−4	5e−5
PSALM_{35}	10M	47M	5e−4	5e−5
PSALM_{8}	5M	29M	5e−4	5e−5
PSALM_{OH}	56M	153M	1e−4	1e−5
PSALM_{FF}	11M	60M	5e−4	5e−5

Table 2: Number of parameters and learning rates (LR) for PSALM models.

5.2 Implementation Details

Both PSALM and PSALM-onehot are trained using cross entropy loss over the entire sequence for both family and clan annotations. For training all PSALM+ESM-2 models, we use ADAM optimizer (Kingma & Ba, 2014) with initial learning rate $5\text{e}{-4}$ for the clan model and $5\text{e}{-5}$ for the family model. These values were selected via hyperparameter tuning from across the following learning rates: $[1\text{e}{-3}, 5\text{e}{-4}, 1\text{e}{-4}, 5\text{e}{-5}, 1\text{e}{-5}]$. A similar hyperparameter search results in a learning rate of $1\text{e}{-4}$ for the PSALM_{OH} clan model and $1\text{e}{-5}$ for the family model. We employ a learning rate scheduler that reduces the learning rate by a factor of $\sqrt{10}$ if the validation loss fails to decrease over consecutive epochs with an additional early stopping criterion of 5 epochs with no improvement. The effective batch size is 32,768 tokens. We assess the model capacity of PSALM by evaluating performance across different model sizes, using the 8M, 35M, 150M, and 650M parameter ESM-2 models denoted as PSALM_{8}, PSALM_{35}, PSALM_{150}, and PSALM_{650}.

The number of parameters for all PSALM clan and family models are given in Table 2. All models were trained on four NVIDIA A100 80GB GPUs. To accommodate memory limitations on the GPU, all sequences are truncated to a maximum length of 4096 residues. This truncation strategy only applies to approximately 0.25% of sequences across the training and test sets and does not reflect a model limitation – PSALM can be used to annotate sequences of any length provided enough memory. All procedures from the HMMER tool suite use version 3.4 (Eddy, 2011). Runtime benchmarking of PSALM_{650} against HMMER* on all test subsets (Table 4; Appendix A.2) demonstrates PSALM annotates the test subsets 5-13x faster than HMMER* but has significantly higher peak memory requirements of 39GB compared to HMMER*'s 0.35GB.

5.3 Metrics

Protein sequence databases have vastly more negatives than positives, requiring extremely low (essentially zero) and controllable false positive rates (FPR), as false annotations are amplified and propagated to additional sequences by later searches. Methods in this field are typically benchmarked for the sensitivity or true positive rate (TPR) they can achieve at a high specificity (low FPR). We also report the F1 score and Matthews Correlation Coefficient (MCC). Here, FPR is defined as the fraction of true negative residues (shuffled, preserving residue composition) incorrectly identified as homologous to a Pfam protein domain family, and TPR is defined as the fraction of residues in ground truth domains correctly identified. We emphasize that we report *per-residue*, not per-domain, metrics.

5.4 Evaluation

We highlight the key observations from the sequence annotation benchmark (Table 3). PSALM_{650} demonstrates superior performance in residue-level domain annotation, accurately annotating a substantial portion of true domain regions while consistently calling fewer false positives compared to HMMER*. Specifically, PSALM_{650} reaches higher TPR, F1 and MCC scores at a lower FPR than HMMER*, with the single exception being family TPR at the 20-40% max PID range test subset. The performance of PSALM_{650} is especially noteworthy in the 0-20% max PID range test subset, which constitutes the most difficult to detect domains in MDPH-Bench, as these sequences share very little max sequence similarity with any domain in the training set – PSALM_{650} is much more sensitive

Table 3: PSALM MDPH-Bench residue-level domain annotation results

PID	Model	Clan				Family			
		TPR	FPR	F1	MCC	TPR	FPR	F1	MCC
0-20%	HMMER*	0.694	0.033	0.819	0.642	0.659	0.033	0.810	0.636
	$PSALM_{650}$	**0.944**	**0.022**	**0.985**	**0.957**	0.750	**0.012**	**0.978**	**0.947**
	$PSALM\_F_{650}$	0.701	0.015	0.827	0.664	0.632	0.015	0.811	0.653
	$PSALM_{FF}$	0.906	0.025	0.976	0.935	**0.767**	0.014	0.966	0.919
	$PSALM_{OH}$	0.490	0.100	0.764	0.559	0.089	0.022	0.236	0.203
20-40%	HMMER*	0.907	0.043	0.941	0.862	**0.876**	0.043	0.939	0.861
	$PSALM_{650}$	**0.966**	**0.020**	**0.985**	**0.964**	0.845	0.015	**0.982**	**0.959**
	$PSALM\_F_{650}$	0.781	0.011	0.878	0.764	0.747	**0.011**	0.873	0.760
	$PSALM_{FF}$	0.933	0.023	0.979	0.951	0.845	0.016	0.975	0.945
	$PSALM_{OH}$	0.516	0.107	0.780	0.602	0.102	0.023	0.282	0.251
40-60%	HMMER*	0.951	0.058	0.957	0.898	0.921	0.058	0.956	0.896
	$PSALM_{650}$	**0.977**	**0.020**	**0.986**	**0.966**	**0.924**	0.017	**0.984**	**0.964**
	$PSALM\_F_{650}$	0.833	0.012	0.906	0.810	0.816	**0.012**	0.904	0.809
	$PSALM_{FF}$	0.964	0.022	0.982	0.957	0.921	0.018	0.981	0.955
	$PSALM_{OH}$	0.666	0.104	0.835	0.671	0.159	0.029	0.430	0.363
60-80%	HMMER*	0.974	0.059	0.971	0.924	0.946	0.059	0.970	0.923
	$PSALM_{650}$	**0.984**	**0.018**	**0.988**	**0.970**	**0.957**	0.016	**0.988**	**0.968**
	$PSALM\_F_{650}$	0.888	0.012	0.938	0.857	0.876	**0.012**	0.937	0.856
	$PSALM_{FF}$	0.977	0.021	0.986	0.962	0.952	0.018	0.985	0.960
	$PSALM_{OH}$	0.788	0.094	0.890	0.745	0.216	0.027	0.573	0.478
80-100%	HMMER*	0.977	0.051	0.972	0.935	0.950	0.051	0.971	0.934
	$PSALM_{650}$	**0.981**	**0.015**	**0.986**	**0.969**	**0.967**	0.012	**0.986**	**0.968**
	$PSALM\_F_{650}$	0.892	0.010	0.940	0.875	0.887	**0.010**	0.939	0.875
	$PSALM_{FF}$	0.975	0.017	0.983	0.961	0.961	0.014	0.982	0.959
	$PSALM_{OH}$	0.877	0.066	0.925	0.836	0.282	0.018	0.709	0.630

and specific than HMMER*. Additionally, $PSALM_{650}$ outperforms all other models in every metric at the clan-level across all PID categories. Our results on model capacity (Table 5; Appendix A.3) demonstrate that PSALM performance increases with model size until $PSALM_{650}$, which is the only model that is competitive with HMMER*.

$PSALM_{OH}$, the baseline to ablate the significance of the ESM-2 contextual residue-level embeddings performs poorly at the family level across all PID categories, though it has a consistently low FPR, and $PSALM_F$. Without the intermediate clan predictions, $PSALM\_F_{650}$ is only competitive with HMMER* at the clan level for the 0-20% max PID range test subset, though $PSALM\_F_{650}$ achieves the lowest max FPR across most test subsets, suggesting that the hierarchical approach leads to a consistent performance gain across PID categories and model sizes (Table 6; Appendix A.4). $PSALM_{FF}$ achieves the best TPR on the 0-20% PID test set and achieves competitive TPR in all PID categories to $PSALM_{650}$, which achieves higher F1 and MCC scores in all PID categories. Both of these pLM-based residue-level domain annotation methods achieve superior performance over HMMER*.

6 EXAMPLES

In Figure 3, we compare the $PSALM_{650}$ and HMMER* annotations to the ground truth annotations determined by HMMER, focusing on three protein sequences drawn from the 0-20% PID test subset, which contains the domains most distantly related to those in the training set.

PSALM is able to identify domains in this test subset that HMMER* either misidentifies (Fig. 3 A) or fails to identify (Fig. 3 B). The nucleoporin domain-containing protein example (Fig. 3 B) demonstrates both PSALM's ability to identify multiple domains in a single input sequence and a limitation to PSALM's high sensitivity – the pink Nucleoporin_C domain is too diverged from related domains in the training set for PSALM to identify the entire length of the domain. The

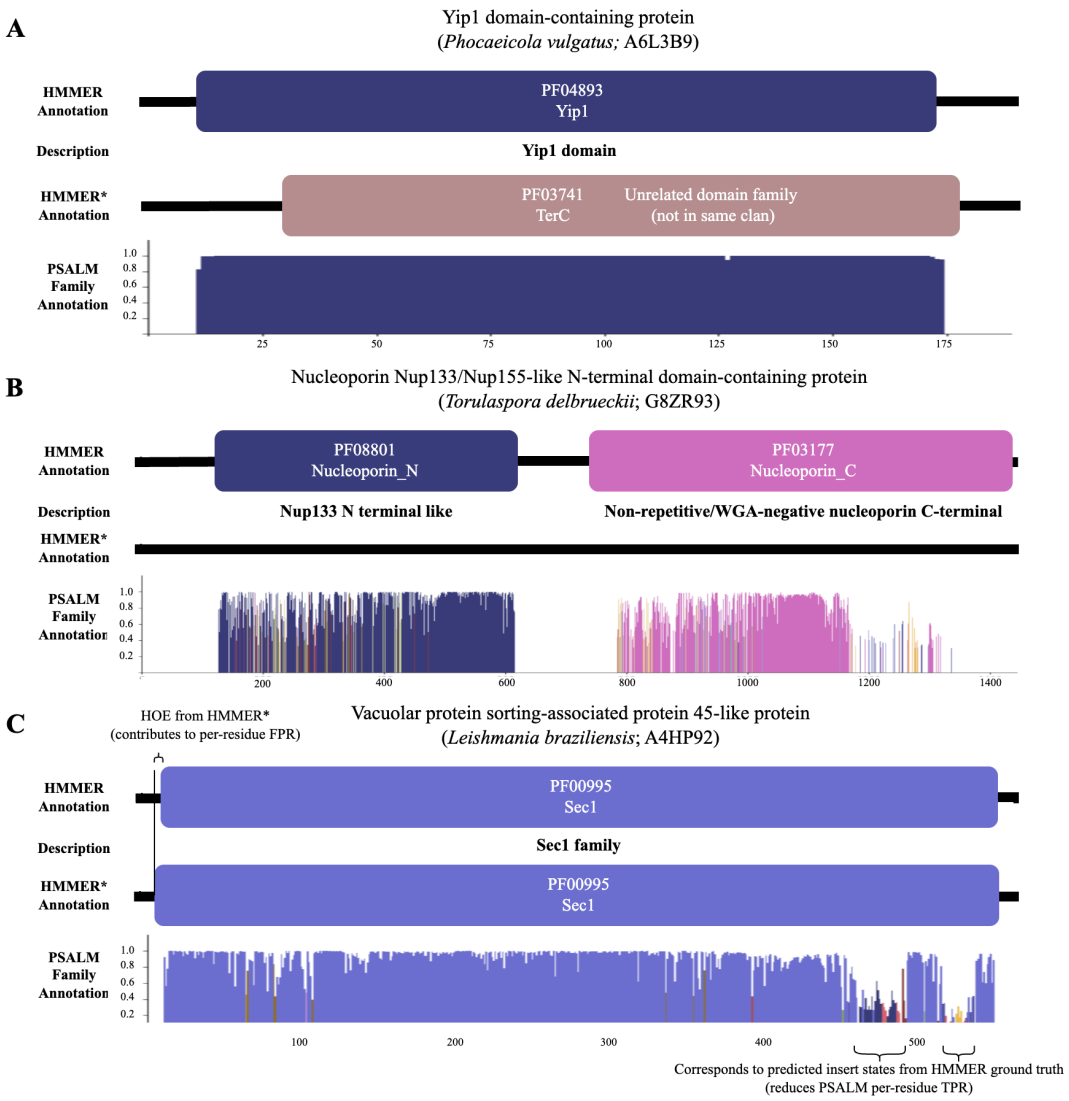

Figure 3: **Comparison of PSALM and HMMER* annotations to the ground truth HMMER annotations for three selected protein sequences from the 0-20% PID test subset.**

vacuolar protein example (Fig. 3 C) highlights two key difficulties in per-residue sensitivity and specificity evaluations. Both PSALM and HMMER* correctly identify the Sec1 domain, but both methods yield different per-residue TPRs and FPRs. HMMER* annotates the domain boundary starting a few residues earlier than the ground truth annotation. This phenomenon is referred to as homologous over-extension (HOE) (Gonzalez & Pearson, 2010), where correct domain assignments may extend for a few residues beyond the precise domain boundary determined in our ground truth annotations, resulting in an increase in per-residue FPR. This would not correspond to an increase in domain-level FPR, as HMMER* almost exactly recreates the ground truth annotation. Without explicit domain-calling on top of the residue-level predictions, it is difficult to separate HOE from completely erroneous annotations in per-residue metrics. The lack of a domain-calling algorithm can also impact PSALM's metrics. PSALM predicts the Sec1 domain correctly at all residues except the two regions with low probability annotations indicated in Fig. 3 B, which reduce PSALM's per-residue TPR. However, these two regions correspond to insert states (insertions in the vacuolar protein relative to the Sec1 domain family alignment) in the raw output of the HMMER ground truth

annotation and would presumably be "smoothed" over with a domain-calling algorithm, ultimately recreating the HMMER annotation.

7 CONCLUSIONS

We introduce PSALM, a highly sensitive and specific pLM-based protein sequence annotation method. PSALM extends the capabilities of self-supervised pLMs with just a few hundred thousand protein sequences, enabling interpretable residue-level annotations at both the clan and family levels. Comparisons with InterPro show PSALM's ability to detect multiple domains, including those currently unannotated. Ablation experiments confirm the importance of pLM embeddings over one-hot encodings and the importance of clan annotations in achieving higher family-level sensitivity and specificity. We find that PSALM performance improves with larger ESM-2 models. The surprising performance of PSALM_{FF} (pLM + FFNN), comparable to PSALM_{650} (pLM + BiLSTM + FFNN), implies that residue embeddings from large pre-trained pLMs like ESM-2 strongly encode residue-level domain membership information. Both PSALM_{650} and PSALM_{FF} outperform HMMER, the state-of-the-art profile-HMM based method for protein domain sequence annotation. We also introduce MDPH-Bench, the first protein sequence benchmark that splits training and test sequences by domain-level sequence similarity for multi-domain proteins. This benchmark minimizes data leakage and enables model evaluation across an evolutionarily-diverse set of proteins.

We provide implementations of the PSALM_{650} family and clan models in a Python package and make all code, data, and benchmark splits used in this work available in our public GitHub repository to support reproducibility and further research in protein sequence annotation.

8 LIMITATIONS & FUTURE WORK

8.1 DATA LEAKAGE

Despite our efforts to mitigate it, information from the test set may still contribute to training through the millions of sequences used to train ESM-2. While we exclude sequences used to train ESM-2 from our test subset with the lowest maximum PID, indirect leakage through homology remains a possibility. For instance, having established that ESM-2 embeddings encode residue-level domain membership, ESM-2 may infer remote homology through embeddings learned from sequences outside of benchmark training set, violating the 0-20% max PID guarantee. Consider a scenario where sequence A and sequence D are a pair of remote homologs with <20% identity. The homology between these sequences could be inferred via intermediate sequences B and C, which are not remote homologs. Even if sequences B and C are not present in MDPH-Bench, ESM-2 was trained on all these sequences and may encode contextual domain information linking residues from A, B, and C. Consequently, embeddings from ESM-2 could violate MDPH-Bench's guarantee of 0-20 PID between sequences A and D, leading to data leakage and/or memorization. Ideally, retraining ESM-2 from scratch on our training data would provide better insight into the out-of-distribution generalization capabilities of PSALM. We have not done this in the present work because of the compute demand for training a pLM like ESM-2, but we plan to rigorously split a much larger set of proteins to train a pLM from scratch.

8.2 DOMAIN CALLING

PSALM cannot distinguish between repeated domains occurring consecutively or accurately resolve split domains. For example, if a domain repeats immediately after itself, PSALM labels the entire two domain block instead of recognizing two separate domains within it. Similarly, when a domain is split, PSALM identifies the two halves as separate domains from the same family, rather than as originating from a single domain. We aim to address this by explicitly modeling the domain boundaries and developing domain-calling algorithms. As mentioned previously, explicit domain calling is necessary to separate the two error modes that contribute to the overall residue-level FPR – incorrect domain assignment and HOE – and we aim to characterize these different error modes in our evaluations once we implement domain calling.

REFERENCES

Tristan Bepler and Bonnie Berger. Learning the protein language: Evolution, structure, and function. *Cell Systems*, 12(6):654–669, 2021.

Maxwell L Bileschi, David Belanger, Drew H Bryant, Theo Sanderson, Brandon Carter, D Sculley, Alex Bateman, Mark A DePristo, and Lucy J Colwell. Using deep learning to annotate the protein universe. *Nature Biotechnology*, 40(6):932–937, 2022.

Yue Cao and Yang Shen. TALE: Transformer-based protein function Annotation with joint sequence–Label Embedding. *Bioinformatics*, 37(18):2825–2833, 2021.

Natalie Dawson, Ian Sillitoe, Russell L Marsden, and Christine A Orengo. The classification of protein domains. *Bioinformatics: Volume I: Data, Sequence Analysis, and Evolution*, pp. 137–164, 2017.

Jacob Devlin, Ming-Wei Chang, Kenton Lee, and Kristina Toutanova. BERT: Pre-training of Deep Bidirectional Transformers for Language Understanding. *arXiv preprint arXiv:1810.04805*, 2018.

Tobias Doerks, Amos Bairoch, and Peer Bork. Protein annotation: detective work for function prediction. *Trends in Genetics*, 14(6):248–250, 1998.

Richard Durbin, Sean R Eddy, Anders Krogh, and Graeme Mitchison. *Biological sequence analysis: Probabilistic models of proteins and nucleic acids*. Cambridge university press, 1998.

Sean R. Eddy. Profile hidden Markov models. *Bioinformatics (Oxford, England)*, 14(9):755–763, 1998.

Sean R Eddy. Accelerated Profile HMM Searches. *PLoS Computational Biology*, 7(10):e1002195, 2011.

Ahmed Elnaggar, Michael Heinzinger, Christian Dallago, Ghalia Rehawi, Yu Wang, Llion Jones, Tom Gibbs, Tamas Feher, Christoph Angerer, Martin Steinegger, et al. Prottrans: Toward Understanding the Language of Life Through Self-Supervised Learning. *IEEE transactions on pattern analysis and machine intelligence*, 44(10):7112–7127, 2021.

EMBL-EBI. Protein Classification: What Are Protein Domains? `https://www.ebi.ac.uk/training/online/courses/protein-classification-intro-ebi-resources/protein-classification/what-are-protein-domains/`, 2024.

Robert D Finn, Jaina Mistry, Benjamin Schuster-Böckler, Sam Griffiths-Jones, Volker Hollich, Timo Lassmann, Simon Moxon, Mhairi Marshall, Ajay Khanna, Richard Durbin, et al. Pfam: clans, web tools and services. *Nucleic Acids Research*, 34(suppl_1):D247–D251, 2006.

Mileidy W Gonzalez and William R Pearson. Homologous over-extension: a challenge for iterative similarity searches. *Nucleic Acids Research*, 38(7):2177–2189, 2010.

Tymor Hamamsy, James T Morton, Robert Blackwell, Daniel Berenberg, Nicholas Carriero, Vladimir Gligorijevic, Charlie EM Strauss, Julia Koehler Leman, Kyunghyun Cho, and Richard Bonneau. Protein remote homology detection and structural alignment using deep learning. *Nature Biotechnology*, pp. 1–11, 2023.

Michael Heinzinger, Maria Littmann, Ian Sillitoe, Nicola Bordin, Christine Orengo, and Burkhard Rost. Contrastive learning on protein embeddings enlightens midnight zone. *NAR Genomics and Bioinformatics*, 4(2):lqac043, 2022.

Sepp Hochreiter and Jürgen Schmidhuber. Long short-term memory. *Neural Computation*, 9(8): 1735–1780, 1997.

Jiajun Hong, Yongchao Luo, Yang Zhang, Junbiao Ying, Weiwei Xue, Tian Xie, Lin Tao, and Feng Zhu. Protein functional annotation of simultaneously improved stability, accuracy and false discovery rate achieved by a sequence-based deep learning. *Briefings in Bioinformatics*, 21(4): 1437–1447, 2020.

L Steven Johnson, Sean R Eddy, and Elon Portugaly. Hidden Markov model speed heuristic and iterative HMM search procedure. *BMC Bioinformatics*, 11:1–8, 2010.

David T Jones. Setting the standards for machine learning in biology. *Nature Reviews Molecular Cell Biology*, 20(11):659–660, 2019.

John Jumper, Richard Evans, Alexander Pritzel, Tim Green, Michael Figurnov, Olaf Ronneberger, Kathryn Tunyasuvunakool, Russ Bates, Augustin Žídek, Anna Potapenko, et al. Highly accurate protein structure prediction with AlphaFold. *Nature*, 596(7873):583–589, 2021.

Kamil Kaminski, Jan Ludwiczak, Kamil Pawlicki, Vikram Alva, and Stanislaw Dunin-Horkawicz. pLM-BLAST: distant homology detection based on direct comparison of sequence representations from protein language models. *Bioinformatics*, 39(10):btad579, 2023.

Samuel Karlin and Stephen F Altschul. Methods for assessing the statistical significance of molecular sequence features by using general scoring schemes. *Proceedings of the National Academy of Sciences*, 87(6):2264–2268, 1990.

Diederik P Kingma and Jimmy Ba. Adam: A Method for Stochastic Optimization. *arXiv preprint arXiv:1412.6980*, 2014.

Maxat Kulmanov and Robert Hoehndorf. DeepGOPlus: improved protein function prediction from sequence. *Bioinformatics*, 36(2):422–429, 2020.

Zeming Lin, Halil Akin, Roshan Rao, Brian Hie, Zhongkai Zhu, Wenting Lu, Nikita Smetanin, Robert Verkuil, Ori Kabeli, Yaniv Shmueli, et al. Evolutionary-scale prediction of atomic-level protein structure with a language model. *Science*, 379(6637):1123–1130, 2023.

Joshua Meier, Roshan Rao, Robert Verkuil, Jason Liu, Tom Sercu, and Alex Rives. Language models enable zero-shot prediction of the effects of mutations on protein function. *Advances in Neural Information Processing Systems*, 34:29287–29303, 2021.

Jaina Mistry, Sara Chuguransky, Lowri Williams, Matloob Qureshi, Gustavo A Salazar, Erik LL Sonnhammer, Silvio CE Tosatto, Lisanna Paladin, Shriya Raj, Lorna J Richardson, et al. Pfam: The protein families database in 2021. *Nucleic Acids Research*, 49(D1):D412–D419, 2021.

Vamsi Nallapareddy, Nicola Bordin, Ian Sillitoe, Michael Heinzinger, Maria Littmann, Vaishali P Waman, Neeladri Sen, Burkhard Rost, and Christine Orengo. CATHe: detection of remote homologues for CATH superfamilies using embeddings from protein language models. *Bioinformatics*, 39(1):btad029, 2023.

Arun Prasad Pandurangan, Jonathan Stahlhacke, Matt E Oates, Ben Smithers, and Julian Gough. The SUPERFAMILY 2.0 database: a significant proteome update and a new webserver. *Nucleic Acids Research*, 47(D1):D490–D494, 2019.

Typhaine Paysan-Lafosse, Matthias Blum, Sara Chuguransky, Tiago Grego, Beatriz Lázaro Pinto, Gustavo A Salazar, Maxwell L Bileschi, Peer Bork, Alan Bridge, Lucy Colwell, et al. InterPro in 2022. *Nucleic Acids Research*, 51(D1):D418–D427, 2023.

William R Pearson. Flexible sequence similarity searching with the FASTA3 program package. *Bioinformatics Methods and Protocols*, pp. 185–219, 1999.

William R Pearson. An Introduction to Sequence Similarity ("Homology") Searching. *Current Protocols in Bioinformatics*, 42(1):3–1, 2013.

Samantha Petti and Sean R Eddy. Constructing benchmark test sets for biological sequence analysis using independent set algorithms. *PLOS Computational Biology*, 18(3):e1009492, 2022.

Chris P Ponting and Ewan Birney. Protein sequence analysis and domain identification. *The Proteomics Protocols Handbook*, pp. 527–541, 2005.

Roshan Rao, Joshua Meier, Tom Sercu, Sergey Ovchinnikov, and Alexander Rives. Transformer protein language models are unsupervised structure learners. In *International Conference on Learning Representations*, 2020.

Michael Remmert, Andreas Biegert, Andreas Hauser, and Johannes Söding. HHblits: lightning-fast iterative protein sequence searching by HMM-HMM alignment. *Nature Methods*, 9(2):173–175, 2012.

Burkhard Rost. Twilight zone of protein sequence alignments. *Protein Engineering*, 12(2):85–94, 1999.

Achille Salaün, Yohan Petetin, and François Desbouvries. Comparing the modeling powers of RNN and HMM. In *2019 18th IEEE International Conference on Machine Learning and Applications*, pp. 1496–1499. IEEE, 2019.

Chris Sander and Reinhard Schneider. Database of homology-derived protein structures and the structural meaning of sequence alignment. *Proteins: Structure, Function, and Bioinformatics*, 9 (1):56–68, 1991.

Theo Sanderson, Maxwell L Bileschi, David Belanger, and Lucy J Colwell. ProteInfer, deep neural networks for protein functional inference. *elife*, 12:e80942, 2023.

Johannes Söding and Michael Remmert. Protein sequence comparison and fold recognition: progress and good-practice benchmarking. *Current Opinion in Structural Biology*, 21(3):404–411, 2011.

Baris E Suzek, Yuqi Wang, Hongzhan Huang, Peter B McGarvey, Cathy H Wu, and UniProt Consortium. UniRef clusters: a comprehensive and scalable alternative for improving sequence similarity searches. *Bioinformatics*, 31(6):926–932, 2015.

Paul D Thomas, Dustin Ebert, Anushya Muruganujan, Tremayne Mushayahama, Laurent-Philippe Albou, and Huaiyu Mi. PANTHER: Making genome-scale phylogenetics accessible to all. *Protein Science*, 31(1):8–22, 2022.

UniProt Consortium. UniProt: the Universal Protein Knowledgebase in 2023. *Nucleic Acids Research*, 51(D1):D523–D531, 2023.

Michel Van Kempen, Stephanie S Kim, Charlotte Tumescheit, Milot Mirdita, Jeongjae Lee, Cameron LM Gilchrist, Johannes Söding, and Martin Steinegger. Fast and accurate protein structure search with Foldseek. *Nature Biotechnology*, 42(2):243–246, 2024.

Ian Walsh, Gianluca Pollastri, and Silvio CE Tosatto. Correct machine learning on protein sequences: a peer-reviewing perspective. *Briefings in Bioinformatics*, 17(5):831–840, 2016.

Ian Walsh, Dmytro Fishman, Dario Garcia-Gasulla, Tiina Titma, Gianluca Pollastri, Jennifer Harrow, Fotis E Psomopoulos, and Silvio CE Tosatto. DOME: recommendations for supervised machine learning validation in biology. *Nature Methods*, 18(10):1122–1127, 2021.

T Wessels and Christian W Omlin. Refining hidden Markov models with recurrent neural networks. In *Proceedings of the IEEE-INNS-ENNS International Joint Conference on Neural Networks. IJCNN 2000. Neural Computing: New Challenges and Perspectives for the New Millennium*, volume 2, pp. 271–276. IEEE, 2000.

Ronald J Williams and David Zipser. A Learning Algorithm for Continually Running Fully Recurrent Neural Networks. *Neural Computation*, 1(2):270–280, 1989.

A Appendix

A.1 Benchmark Creation

A.1.1 BLUE

We use the BLUE algorithm (Petti & Eddy, 2022) to split the 1.2M Pfam Seed domains into preliminary train and test sets with a PID threshold of 25%. The pairwise PID between two sequences $\mathbf{x}$ and $\mathbf{y}$ is defined as follows:

$$\text{PID}(\mathbf{x}, \mathbf{y}) = \frac{\text{\# aligned residues}}{\min(\ell(\mathbf{x}), \ell(\mathbf{y}))}, \tag{4}$$

where $\ell(\mathbf{x})$ and $\ell(\mathbf{y})$ represent the lengths of sequences $\mathbf{x}$ and $\mathbf{y}$, respectively. If two domains are in the same family, PID is directly calculated from their seed alignment. If two domains are not in the same family but are in the same clan, they are aligned using the `glsearch` tool from the FASTA3 software package (Pearson, 1999), which performs a "global-local" alignment to account for possible large differences in sequence length. If two domains are not in the same clan, they are assumed to share $< 25\%$ PID.

A.1.2 Ground Truth Annotation

We determine "ground truth" by annotating full length sequence with Pfam Seed profile HMMs using `hmmscan` with strict inclusion criteria (E-value < 0.001, bitscore ≥ 30). The highest-scoring annotation at each residue is taken as ground truth, but additional post-processing is necessary to ensure that "nested" domain structures are retained. This is accomplished by considering the "match strings" that HMMER generates for an alignment. The match strings contain characters that represent matches, where residues align to a given domain profile, and characters that represent inserts, where unaligned residues are inserted into the sequence relative to the domain profile. Annotating the highest-scoring match state at each residue preserves nested domain structure in the ground truth annotations (Fig. 4).

In a match string, regions with majority matches may contain a few inserts and vice versa. To prevent frequently alternating annotations in the ground truth, we smooth the match and insert states in the

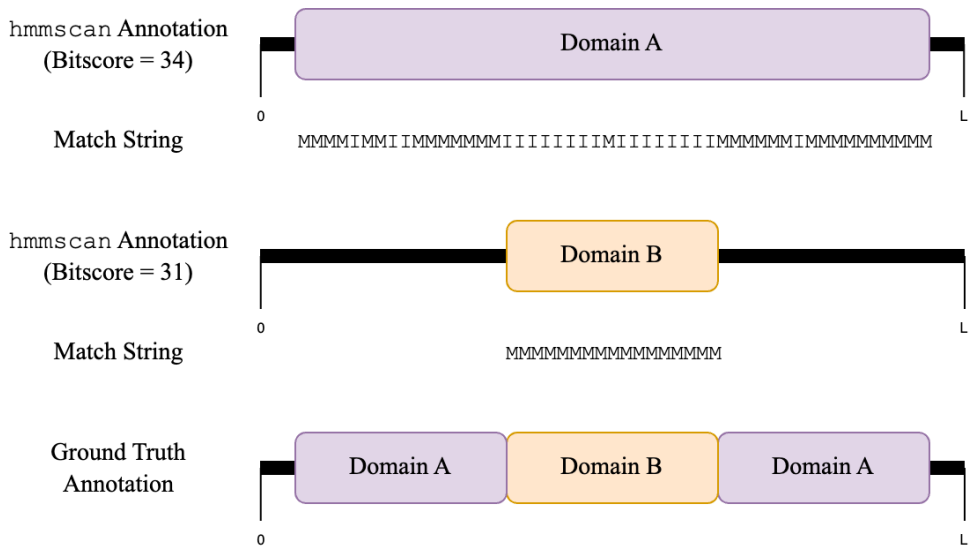

Figure 4: **A schematic of nested domains with two domains A and B in the nested format A-B-A.** As A is annotated with a higher score than B and overlaps with B, annotating residues only via highest score will fail to include domain B. Using the match state strings to identify smoothed maximal segments preserves the nested domain structure in the ground truth annotation.

match string by identifying maximal scoring segments within the sequence. We assign insert states a positive score and match states a negative score. The segment of the sequence with the greatest aggregate score is known as the maximal segment (Karlin & Altschul, 1990), and all residues in the maximal segment are denoted as insert states. The scores s_i for each state are inferred from the match string for a given sequence:

$$s_i \propto \log\left(\frac{q_i}{p_i}\right), \tag{5}$$

where p_i is the frequency with which the state appears in the match string, and q_i is a state's target frequency, with $\sum_i p_i = 1$ and $\sum_i q_i = 1$. We set the insert state target frequency at 0.85, the match state target frequency at 0.15, and the length threshold at 20, below which maximal segments are ignored.

A.1.3 Maximum PID Calculation

Once the full length test sequences have been retrieved and subsequently filtered, we compute, for each test sequence, the maximum PID between any of its annotated domains and any annotated domain in train via Algorithm 1. Each test sequence is assigned to a single (out of five) test subset based on its maximum PID.

Algorithm 1 Percent identity splitting test set

Require: train sequences $\mathcal{D}^{tr}$, test sequences $\mathcal{D}^{te}$, Pfam family profile HMMs $\mathcal{F}$
  Initialize an empty dictionary-like structure record_max_pids
  for $f \in \mathcal{F}$ **do** ▷ identify domains belonging to family f
    train_domains ← `hmmsearch` f against $\mathcal{D}^{tr}$
    test_domains ← `hmmsearch` f against $\mathcal{D}^{te}$
    for (domain,sequence_id) ∈ test_domains **do** ▷ find max PID b/w test domain and train
      MSA ← `hmmalign` domain to train_domains with f
      domain_pids ← `esl-alipid` MSA
      max_pid ← max(domain_pids)
      if sequence_id not in record_max_pids **then** ▷ Label sequence with max domain PID
        record_max_pids[sequence_id] ← max_pid
      else if max_pid > record_max_pids[sequence_id] **then**
        record_max_pids[sequence_id] ← max_pid
      end if
    end for
  end for
  Assign each sequence in $\mathcal{D}^{te}$ to a test split based on max pid

The `esl-alipid` tool calculates PID for all pairs of sequences for a given MSA, and is part of the EASEL software package, which can be downloaded together with HMMER (Eddy, 2011).

A.2 Runtime Benchmarking

Runtimes are recorded as total (wall clock) time. All HMMER* timings were measured on a single core on a dedicated cluster node. Additionally, the PSALM_{650} is run on a single NVIDIA A100 GPU with 80GB memory.

Table 4: Memory and runtime usage for $PSALM_{650}$ and HMMER* across PID categories.

Test Subset	0-20%	20-40%	40-60%	60-80%	80-100%
# Sequences	4,087	37,319	17,446	8,570	5,864
Average Length	399.55	409.47	617.95	774.33	1,044.7
$PSALM_{650}$ Peak Mem (GB)	22.49	38.49	34.97	36.46	29.74
$PSALM_{650}$ Time (s)	99.88	815.39	662.97	451.03	488.36
HMMER* Peak Mem (GB)	0.18	0.35	0.27	0.24	0.21
HMMER* Time (s)	1,330	10,805	5,802	3,119	2,403

A.3 Model Capacity Experiments

We assess the model capacity of PSALM by evaluating performance across different model sizes, using the 8M, 35M, 150M, and 650M parameter ESM-2 models denoted as $PSALM_8$, $PSALM_{35}$, $PSALM_{150}$, and $PSALM_{650}$ (Table 5.

Table 5: PSALM model capacity results on MDPH-Bench

		Clan				Family			
PID	Model	TPR	FPR	F1	MCC	TPR	FPR	F1	MCC
0-20%	HMMER*	0.694	0.033	0.819	0.642	0.659	0.033	0.810	0.636
	$PSALM_{650}$	**0.944**	**0.022**	**0.985**	**0.957**	**0.750**	**0.012**	**0.978**	**0.947**
	$PSALM_{150}$	0.862	0.133	0.912	0.758	0.621	0.050	0.869	0.730
	$PSALM_{35}$	0.729	0.174	0.847	0.620	0.428	0.071	0.721	0.532
	$PSALM_8$	0.589	0.214	0.772	0.488	0.211	0.079	0.463	0.293
	$PSALM_{OH}$	0.490	0.100	0.764	0.559	0.089	0.022	0.236	0.203
20-40%	HMMER*	0.907	0.043	0.941	0.862	**0.876**	0.043	0.939	0.861
	$PSALM_{650}$	**0.966**	**0.020**	**0.985**	**0.964**	0.845	**0.015**	**0.982**	**0.959**
	$PSALM_{150}$	0.887	0.092	0.925	0.819	0.727	0.036	0.910	0.817
	$PSALM_{35}$	0.799	0.131	0.873	0.709	0.607	0.056	0.825	0.682
	$PSALM_8$	0.636	0.192	0.788	0.553	0.353	0.074	0.623	0.452
	$PSALM_{OH}$	0.516	0.107	0.780	0.602	0.102	0.023	0.282	0.251
40-60%	HMMER*	0.951	0.058	0.957	0.898	0.921	0.058	0.956	0.896
	$PSALM_{650}$	**0.977**	**0.020**	**0.986**	**0.966**	**0.924**	**0.017**	**0.984**	**0.964**
	$PSALM_{150}$	0.888	0.058	0.927	0.834	0.806	0.026	0.919	0.832
	$PSALM_{35}$	0.826	0.101	0.882	0.736	0.728	0.049	0.866	0.738
	$PSALM_8$	0.704	0.158	0.809	0.598	0.532	0.072	0.741	0.567
	$PSALM_{OH}$	0.666	0.104	0.835	0.671	0.159	0.029	0.430	0.363
60-80%	HMMER*	0.974	0.059	0.971	0.924	0.946	0.059	0.970	0.923
	$PSALM_{650}$	**0.984**	**0.018**	**0.988**	**0.970**	**0.957**	**0.016**	**0.988**	**0.968**
	$PSALM_{150}$	0.912	0.058	0.940	0.850	0.859	0.028	0.936	0.852
	$PSALM_{35}$	0.845	0.083	0.900	0.761	0.782	0.045	0.888	0.759
	$PSALM_8$	0.728	0.154	0.827	0.609	0.605	0.084	0.778	0.583
	$PSALM_{OH}$	0.788	0.094	0.890	0.745	0.216	0.027	0.573	0.478
80-100%	HMMER*	0.977	0.051	0.972	0.935	0.950	0.051	0.971	0.934
	$PSALM_{650}$	**0.981**	**0.015**	**0.986**	**0.969**	**0.967**	**0.012**	**0.986**	**0.968**
	$PSALM_{150}$	0.895	0.049	0.929	0.845	0.851	0.024	0.924	0.845
	$PSALM_{35}$	0.812	0.088	0.872	0.732	0.732	0.046	0.853	0.725
	$PSALM_8$	0.711	0.114	0.809	0.624	0.601	0.059	0.761	0.600
	$PSALM_{OH}$	0.877	0.066	0.925	0.836	0.282	0.018	0.709	0.630

A.4 FAMILY-ONLY PSALM FULL RESULTS

We conduct an additional ablation experiment in order to study the effect of predicting clan-level annotations as an interpretable intermediate in PSALM (Table 6). We retrain the $\text{PSALM}_{\text{size}}$ family model without providing any predicted clan annotations and denote this model as $\text{PSALM\_F}_{\text{size}}$ for all ESM-2 model sizes tested in the main text. Clan predictions are generated by identifying the clan corresponding to the predicted family.

Table 6: Family-only PSALM MDPH-Bench Results

		Clan				Family			
PID	Model	TPR	FPR	F1	MCC	TPR	FPR	F1	MCC
0-20%	HMMER*	0.694	0.033	**0.819**	0.642	**0.659**	0.033	**0.810**	0.636
	PSALM_F_{650}	**0.701**	**0.015**	0.827	**0.664**	0.632	**0.015**	0.811	**0.653**
	PSALM_F_{150}	0.630	0.034	0.781	0.596	0.540	0.034	0.753	0.576
	PSALM_F_{35}	0.560	0.065	0.733	0.523	0.412	0.065	0.670	0.476
	PSALM_F_{8}	0.394	0.115	0.599	0.355	0.232	0.115	0.469	0.253
20-40%	HMMER*	**0.907**	0.043	**0.941**	**0.862**	**0.876**	0.043	**0.939**	**0.861**
	PSALM_F_{650}	0.781	**0.011**	0.878	0.764	0.747	**0.011**	0.873	0.760
	PSALM_F_{150}	0.705	0.032	0.833	0.691	0.651	0.032	0.822	0.682
	PSALM_F_{35}	0.662	0.058	0.800	0.632	0.581	0.058	0.778	0.614
	PSALM_F_{8}	0.479	0.102	0.674	0.462	0.356	0.102	0.605	0.406
40-60%	HMMER*	**0.951**	0.058	**0.957**	**0.898**	**0.921**	0.058	**0.956**	**0.896**
	PSALM_F_{650}	0.833	**0.012**	0.906	0.810	0.816	**0.012**	0.904	0.809
	PSALM_F_{150}	0.785	0.025	0.877	0.759	0.758	0.025	0.873	0.756
	PSALM_F_{35}	0.746	0.048	0.846	0.703	0.708	0.048	0.839	0.697
	PSALM_F_{8}	0.594	0.087	0.749	0.557	0.520	0.087	0.723	0.535
60-80%	HMMER*	**0.974**	0.059	**0.971**	**0.924**	**0.946**	0.059	**0.970**	**0.923**
	PSALM_F_{650}	0.888	**0.012**	0.938	0.857	0.876	**0.012**	0.937	0.856
	PSALM_F_{150}	0.842	0.025	0.910	0.801	0.823	0.025	0.908	0.799
	PSALM_F_{35}	0.792	0.048	0.876	0.733	0.770	0.048	0.872	0.730
	PSALM_F_{8}	0.632	0.093	0.776	0.569	0.586	0.093	0.762	0.558
80-100%	HMMER*	**0.977**	0.051	**0.972**	**0.935**	**0.950**	0.051	**0.971**	**0.934**
	PSALM_F_{650}	0.892	**0.010**	0.940	0.875	0.887	**0.010**	0.939	0.875
	PSALM_F_{150}	0.835	0.024	0.903	0.808	0.819	0.024	0.901	0.806
	PSALM_F_{35}	0.740	0.047	0.839	0.701	0.720	0.047	0.835	0.697
	PSALM_F_{8}	0.661	0.078	0.783	0.609	0.627	0.078	0.774	0.601